VISCOELASTIC BEHAVIOUR AND WET SUPERCONTRACTION OF MAJOR AMPULLATE SILK FIBRES OF CERTAIN ORB-WEB-BUILDING SPIDERS (ARANEAE)

By ROBERT W. WORK

Fiber and Polymer Science Program, North Carolina State University, Raleigh, North Carolina 27695-8302, U.S.A.

SUMMARY

1. The axial retractive stresses that cause the supercontraction of wetted major ampullate silk fibres and the stresses developed upon re-extension from the supercontracted condition are quantified and illustrated.

2. The viscoelastic behaviour of major ampullate silk fibres, subjected to the amounts of elongation that would be produced by a spider on its dragline, is described and illustrated.

3. When major ampullate silk fibres are either wet elongated from supercontraction or when dry from initial lengths, viscoelastic stress relaxations are found to be functions of the logarithms of time. Regression curves illustrate these relationships and normalized results are subjected to statistical analyses.

4. Viscoelastic memory of major ampullate silk fibres is illustrated.

5. The characteristics of viscoelastic stress relaxation and viscoelastic memory of major ampullate silk fibres appear not to be associable with taxonomy.

6. Examples are suggested in which supercontraction and stress relaxation act in the formation and placement of major ampullate silk fibres as structural elements of the orb web.

INTRODUCTION

This study of major ampullate silk fibres (MaAS, singular and plural) of some orb-web-building spiders has three primary objectives: (1) the quantification of stress-strain aspects of the phenomenon of supercontraction (supercontraction, supercontract and variants = SC) of MaAS, (2) the quantification of the stress relaxation behaviour of MaAS in the dry (dry = room-conditioned) and water-wetted states and (3) the application of the observations developed from items 1 and 2 to the placing of these fibres in orb webs.

Key words: Spider, silk, ampullate.

Background

When elastic solids, such as some metals and glass, are subjected to small deformations, Hooke's Law applies; stress is directly proportional to strain and independent of rate of strain. Simple liquids (not polymers or their solutions) obey Newton's Law; the stress being directly proportional to the rate of strain. Organic fibres, of which MaAS are typical, obey neither law, but their responses to deformation relate them to both. Hence, they are viscoelastic bodies. Although the application of this descriptive term to textile fibres is of technical origin, the lay public has always known that the force-elongation behaviour and dimensional recovery therefrom of fibrous compositions are time sensitive. Of the three forms of axial deformation of fibres under externally applied forces (these being extension, torsion and compression), the first has been studied widely, the second to a limited degree and the third virtually not at all.

Attempts to explain and quantify these actions were first reviewed by Leaderman (1943), with a bibliography of 210 references, and with the development of fully synthetic man-made fibres, more studies have now been made (for general reviews see Rebenfeld, 1967; Kargin & Slonimsky, 1968; Ferry, 1969). This paper will consider only the viscoelastic behaviour of MaAS associated with axial extension under externally applied forces, and SC, wherewith the driving force is internal.

Historical: spider silks

It was recognized very early that silk fibres are not elastic bodies. Weber (1835) found that when a load was applied to silk, the axial extension gradually increased as a function of time. When the load was removed, the initial length was not immediately recovered. More recent studies of spider silk have examined their chemical nature and viscoelastic behaviour and in some cases have indicated relationships between these. Analyses of the amino acid compositions of spider silk polypeptides have been made (E. Fischer, 1907; Braunitzer & Wolff, 1955; F. G. Fischer & Brander, 1960; Lucas, Shaw & Smith, 1955, 1958, 1960a,b; Lucas, 1964; Peakall, 1964, 1968; Zemlin, 1968; Andersen, 1970) and show MaAS to be higher in glycine and alanine than other silks (Lucas *et al.* 1960a). On the basis of the molecular model of an anti-parallel pleated (or rippled) sheet, proposed by Pauling & Corey (1951, 1953), now generally accepted for all silks, the preponderance of the small-sized glycine and alanine groups, and the presence of correspondingly fewer large groups on the molecular chains, should determine that MaAS would be extremely strong. That such is the case, has been shown by measurements of force-elongation properties by Benton (1907), Herzog (1915), De Wilde (1943), Lucas *et al.* (1955), Lucas (1964), Zemlin (1968), Denny (1976) and Work (1976, 1977b). Where the more recent papers have illustrated these properties, the curves demonstrate their viscoelastic behaviour up to structural failure. Related information is found in Warwicker's papers on X-ray diffraction (1954, 1955, 1960) which show that the dimensions of the unit cells in crystalline domains of all silks are uniform (1) in their molecular chain axes and (2) in the hydrogen bonding

directions, but differ in the third dimension, that occupied by the side chains. Although ratios of crystalline to amorphous domains (X-ray diffraction definition) have not yet been determined, the presence of the latter domains is implied by Warwicker, as well as being taken for granted by macromolecular theory. [See Iizuka (1965) for crystallinity of silk from *Bombyx mori*.] It is within the amorphous domains that deformations take place at the molecular level; as an oversimplification, the crystalline domains act as non-deformable solids.

Only in recent years have spider fibres been studied specifically from the viewpoint of viscoelastic behaviour, but Benton (1907) demonstrated its existence when describing an 'elastic after effect'. He showed that when spider silks (source and type not described) were axially loaded, the resulting immediate extensions were followed by small continuing extensions over a period of time. When such loads were then removed, the silks retracted to lengths greater than they possessed initially, and continued to retract slowly thereafter. Denny (1976) examined the high modulus frame fibres (presumably MaAS) and the elastomeric (rubber-like), sticky, core elements of the trapping spiral. Ko (1976) prepared a thesis on non-linear viscoelasticity, which included data on spider silk fibres. Wainwright (1976) has discussed both silk and viscoelastic bodies. Work (1978) mentioned the slow increase in length of the draglines supporting spiders, and suggested that its basis would be viscoelastic creep. Eberhard (1981) has noted the importance of viscoelastic behaviour in web construction.

Supercontraction is well known, but not commonplace, among natural and man-made fibres. Although the term has never been defined, it connotes a shrinkage far greater than occurs during the normal usage of textile fibres. It can be induced in wool by treatment with aqueous solutions of sodium sulphide (Speakman, 1931) or steam (Astbury & Woods, 1933). Supercontraction of natural fibres has been reviewed by Whewell & Woods (1946) and by Ebert, Ebert & Wendorff (1970). Studies of the SC of man-made fibres suggest that SC is, to a greater or lesser degree, the reversal of 'drawing', i.e. the step in the industrial production of those fibres in which the 'as spun' fibres are stretched as much as 400 %, to become usable commercial products. (See Uchiyama & Yamamoto, 1972; Prevorsek, Tirpak, Harset & Reimschsiessel, 1974; Melinte, Leanca, Moise & Mateescu, 1977; and Chabert, Nemoz & Valentin, 1979, for recent papers on the subject.) As with wool, SC of man-made fibres have been brought about only by the use of elevated temperature, chemically powerful swelling agents, or both.

In contrast, when axially restrained MaAS are wetted with water at room temperature, radial expansion occurs and axial retractive forces are generated. When unrestrained, these retractive driving forces produce 'instantaneous' SC (Work, 1977*b*), resulting in axially stable lengths (SC ratio = SC length/initial length), these being associable with taxonomy (Work, 1981*b*). The SC fibres may be re-extended in the wetted condition or dried and then re-extended. These several aspects of SC are illustrated in Fig. 1, idealized for MaAS having mean SC ratios of 0·55.

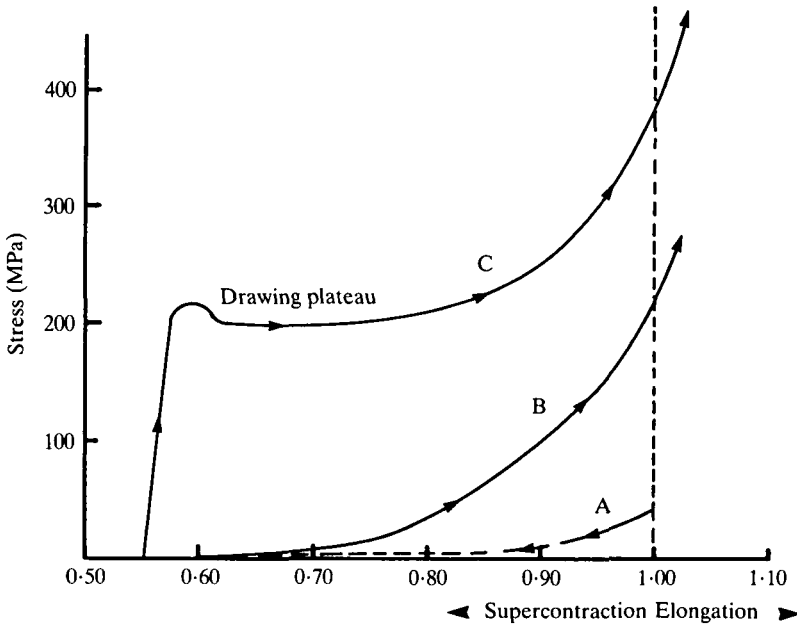The chemically powerful swelling agents, saturated aqueous solutions of

Fig. 1. Curves (idealized) illustrating aspects of supercontraction (SC) of major ampullate silk fibres (MaAS). (A) Wetted and allowed to SC. (B) Elongated from SC in the wet state. (C) Elongated from SC after drying.

NaSCN and LiBr, cause SC to a greater degree than water. LiBr solution produces gellation both in MaAS and minor ampullate silk fibres (MiAS), although these latter fibres do not SC in water (Work & Morosoff, 1982). In an X-ray diffraction study, described in the same paper, it was seen that the crystallites (X-ray diffraction definition) rotate in three dimensional space during SC, but are otherwise unchanged. A mathematical study of SC, as related to changes in birefringences, has been made by Fornes, Work & Morosoff (1983), but a definitive description of the phenomenon from the standpoint of what takes place at the molecular level remains to be developed. Fitzgerald & Willer (1983) found that the silk deposited by the eastern tent caterpillar *Malacosoma americanum* shrinks '... shortly after it is spun ...', but whether this is caused by moisture has not yet been determined.

MATERIAL AND METHODS

Sampling and sample preparation

Samples of MaAS produced by mature females are obtainable from orb webs (Work, 1976, p. 486), draglines (Work, 1978, p. 182), trailing pairs (Work, 1981*a*, pp. 2–3) and by forcible silking (Work & Emerson, 1982). The species providing most of the samples used in this study were *Araneus diadematus* (Clerck), *Araneus gemma* (McCook), *Nuctenea cornuta* (Clerck), *Nuctenea sclopetaria* (Clerck), *Neoscona hentzii* (Ketserling), *Argiope argentata* (Fabricius), *Argiope aurantia*

(Lucas), *Eriophora fuliginea* (C. L. Koch), *Eriophora ravilla* (C. L. Koch), *Nephila clavipes* (Linnaeus) and *Nephilengys cruentata* (Fabricius). (Classification according to H. W. Levi, personal communications, 1980–81.)

Primary samples of MaAS may be secured from webs by direct transfer to microscope slides, but those from draglines and trailing silk are more conveniently first placed on pieces of black (for contrast) poster board from which sections may be transferred to microscope slides. Forcibly taken MaAS must be backwound from the receiving mandrel (Work & Emerson, 1982, Figs 1, 2, 3) onto microscope slides. After placing on a slide tautly, but without stretching, the ends held in place with tiny tabs of self adhesive tape, a sample is examined microscopically (100–430 × magnification) for presence of trapped debris, piriform cemented points (more common than the uninitiated may expect), MiAS (about one-third the diameter of MaAS and often looping slightly away from them), and 'fine' fibres. These last (Work, 1981*a*) are easily missed when in line contact with, and in the cusps of, pairs of MaAS. From a satisfactory primary sample, one subsample is transferred and cemented to another microscope slide for determination of diameter and SC ratio (and birefringence, if needed for other studies). An adjacent subsample is placed over a measured hole cut out of the supporting black poster board, and cemented at the edges of the cutout with a minimal amount of the black, rubber-based cement commonly used in mounting samples for scanning electron microscopy (SEM). This cement does not migrate by capillarity along the fibres, as does catalysed epoxy cement. Advantage is taken of the stronger adhesive property of the latter by coating it over the SEM cement, onto the surrounding poster board, and over the free ends of the MaAS extending back from the SEM cement, care being taken that it does not touch the SEM cement–MaAS interface. Each primary sample on a microscope slide will usually supply two or three lengths in the subsample for optical measurements and SC ratio, and one, often two, samples for use in the Instron device.

Instrumentation

Diameters of MaAS are determined with a Leitz Measuring Device (1250 × magnification) in a Leitz polarizing microscope, using crossed polarizers, a first-order red plate in the optical path, with the fibre axis at 45° to the plane of polarization. For samples used in this study, the coefficient of variation (CV) secured from three replicate measurements is in the range 3–4 %.

Viscoelastic and SC behaviour of MaAS are measured through the use of an Instron tensile measuring machine (hereinafter, Instron). It provides for several selectable constant rates of elongation (extension) as the independent variables and records resulting forces as dependent variables. The essential operating features of this device are illustrated in Fig. 2.

In order that the Instron might be used to make measurements on water-immersed samples, a glass container was constructed in which the lower sample clamp may be placed. This container is tall enough to allow the entire sample to be immersed, up to the upper clamp, and has a dished bottom to facilitate
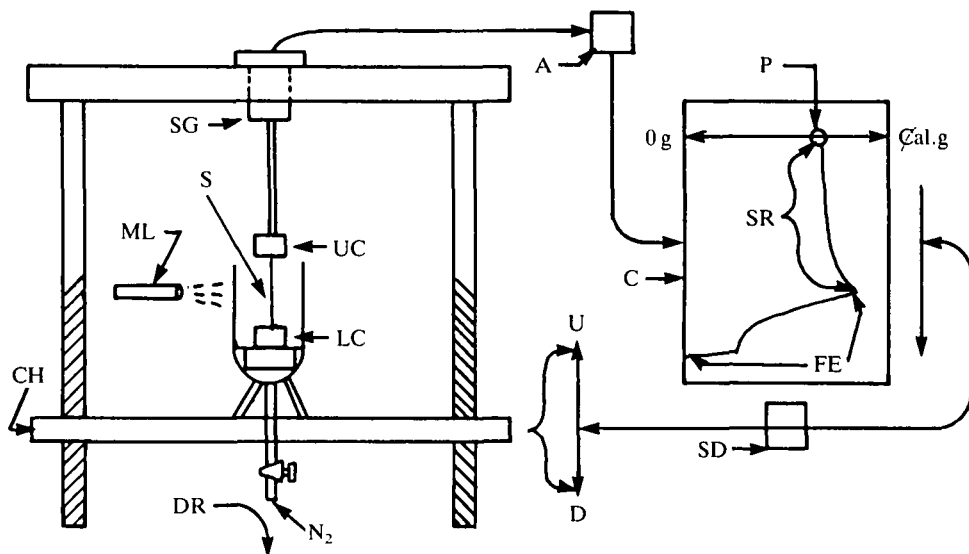
Fig. 2. Essential operating parts of an Instron tensile testing machine. S, sample; LC, lower clamp; UC, upper clamp; SG, strain gauge; CH, moving crosshead; ML, microscope lamp; DR, water drain; N_2, nitrogen; U, crosshead movement up; D, crosshead movement down; A, amplifier; C, chart; P, pen; 0g, zero grams on chart; Cal.g, grams of calibration; SR, stress relaxation curve on chart; FE, force elongation curve on chart; SD, synchronous drive of crosshead and chart and ratio control.

drainage *via* glass tubing carrying a stopcock. After removal of water, a source of dry nitrogen may be connected to the drain line, so as to make possible the rapid and complete drying of the sample, lower clamp and inside of the container.

To mount the sample of MaAS between the lower moving clamp and the upper registering clamp, all excess portions of the poster board sample holder, including one side of the length-determining cutout, are cut away, leaving only one side of the original poster board frame to support the sample. This is placed between the clamps, after which the remaining side of the poster board is severed and entirely removed, thereby leaving the sample as the sole connection between the clamps. All of this manipulation is done so that the now free sample will be slack: stretching must be carefully avoided. By means of minute crosshead adjustments the sample is made taut, but under zero tension. In order to measure stress relaxation in either dry or wetted conditions, the automatic controls of the Instron are set for the desired crosshead speed and limit of extension. The rate of elongation is based on that commonly accepted in the fibre and textile industry, 100 % of sample length per minute. If, however, the elongation would be completed in less than 5 s, a lower crosshead speed is selected, to increase precision. A combination of machine inertia and recording pen lag invalidate the first 3 s of time after theoretical stoppage for an older Instron used in the early part of this study. A new model reduced this to 1 s. (It will be seen later, in Tables 2 and 3, that regression calculations start at one or the other of these time periods.) Chart speeds are selected in order to make the expected inked curves clearly interpretable. With these preparations complete, the

Instron and a digital stop-watch are started simultaneously. As each experiment progresses and the rate of lateral movement of the recording pen decreases, chart speed is stepwise lowered.

If wet stress relaxation or stresses present during SC or elongation therefrom are to be determined, the container in which the lower clamp and its support have been placed is filled with water until its level is as close to the tab in the upper clamp as the experimenter dares to bring it without wetting the tab and clamp. Wetting must be avoided, because although the interfacial tension between MaAS and water is negligible, that tension between water and the large surfaces of tab and clamp will overwhelm the forces to be measured. The SC force is registered the instant that water touches the lower end of the sample. If decreasing SC tension is to be measured, as a function of the decrease in length during SC, the water level is lowered and the crosshead is immediately activated so as to allow retraction in sample length. Upon reaching the SC state, the sample is seen to become bowed. Because the SC sample is dimensionally stable, the straight-bowed transition can be established by minute up and down movements of the crosshead, from which the SC ratio (SC length/initial length) is accurately established. Any time that a wetted sample is extended, water must be added to the container so as to keep the sample wet.

A quite different situation exists when it is desired to measure the elastic memory of a dry sample that has been held in a condition of tension for a day or more to allow stress relaxation to arrive at a very slow rate. Ideally, the Instron crosshead should be activated to reduce the tension rapidly to zero and stop there. This cannot be done. Zero tension is approached in an asymptote-like curve and overshot, at which time the sample is observed to bow. The experimenter requires 30–90 s to manipulate the Instron to secure sample tautness, during which time it is shrinking, due to elastic memory. It follows that the time at which tension can start to be recorded is only a reference for ensuing time-tension data, but not a true zero time for the starting of elastic memory.

There are two fundamental reasons why the measured forces cannot be normalized to units of stress for any viscoelastic fibre, even if the investigator is prepared to determine the cross-sectional areas of individual fibres. During elongation the volumes of these organic fibres do not remain constant. Therefore, the ratio of cross-sectional area to amount of elongation, i.e. the Poisson ratio, is not 0·5. Also, the Poisson ratios of fibres are generally unknown (see Wainwright, 1976, Table 2.2) and even if such a ratio is determined at one level of elongation, it might differ at another. In addition, there are limitations that apply to the MaAS that are the subject of this paper. (1) It has been found (Work, 1984) that the macro structure of MaAS is often radially 'skin-core', a characteristic, when it is present, that can only be known to exist when the skin fractures, concomitant with re-extension from SC in the wetted condition. (2) Another uncertainty is present for water-wetted MaAS. Some information on their radial expansions is available (Work, 1977b), but these measurements exhibit considerable variability and apply only to unstrained samples. For these reasons the experimenter is forced to accept

some less than satisfactory means of converting measured tensions and cross-sectional areas of MaAS (both differing widely from sample to sample) to units of 'stress'. It is possible to use either a Poisson ratio of 0·5 or the cross section(s) of the initial fibre(s) as the basis of calculation, in an effort to allow comparisons to be made among chemically and physically similar materials. In this paper the latter option, i.e. the initial cross-sectional areas of MaAS in the dry, unstrained state are used in all dry and water-wetted conditions of measurements. The liberty taken with the definitions of stress and modulus will not be indicated further in the text.

<div align="center">

RESULTS

Supercontraction and re-extension

</div>

The Instron cannot be used to determine the rate of SC, but it can be used to measure the SC force developed upon wetting when this is greater than the lower uncertainty limit of the device, a condition satisfied only by a pair of MaAS, each of about 2 μm diameter or larger. Thus, in a related study to determine SC ratios (Work, 1981b), out of 101 samples only 65 exhibited measurable SC tensions, the mean SC stress of the latter group being 33 MPa as already seen in Fig. 1. When the diameters of a pair are about 3 μm or larger, the SC forces may be measured as such samples are allowed to retract in length when mounted in the Instron. The example curves of Fig. 3 are shown with dashed lines as the stresses approach zero, due to the uncertainty of machine response at very small tensions. Interpolations are possible because the SC ratios are known, at which points tensions must become zero. Unlike samples in dry conditions, reduced to zero tension from prior measurable tensions (to be described later), SC samples do not develop elastic memory.

The re-extension curves from SC to initial lengths of wetted MaAS differ from the corresponding SC retraction curves, as has been seen in idealized form in Fig. 1. Re-extension curves (Fig. 4) all arrive at their initial lengths at considerably higher stresses than the original SC stresses (Fig. 3). It is to be expected that any force-elongation curves of viscoelastic fibres will vary as functions of time during elongation, as Denny (1976, Fig. 3 and related text) has demonstrated for frame silk of *Nuctenea sclopetaria* (= *Araneus sericatus*) elongated to rupture in a dry condition. But experiments on MaAS, elongated from SC to initial lengths, at rates in the range of 5–100 % of initial lengths per minute, produced variations in stresses that were comparable with variations obtained with replicate measurements on individual samples, when these were elongated at a single rate. Pertinent data relative to the curves seen in Figs 3 and 4 are given in Table 1. The stress relaxation aspects of re-extension curves will be presented in a later section. The areas under the curves seen in Fig. 3 are measures of the potential energy released by the samples during SC, and the areas under the curves in Fig. 4 correspond to the dynamic energy imposed upon the samples when wet extended from SC to initial lengths. These areas were measured by planimeter and are found in
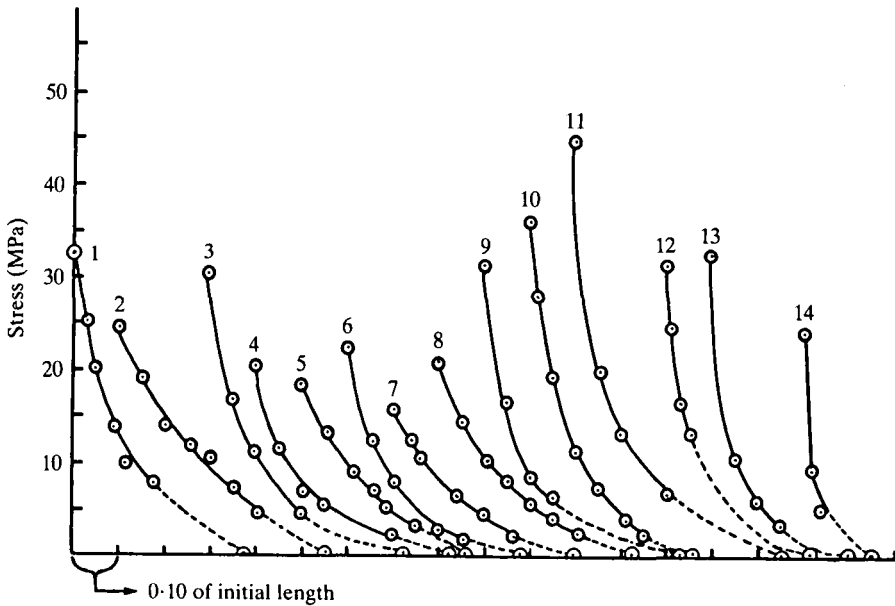
Fig. 3. SC *versus* stress curves. Each SC curve starts from a stress at initial length, above a tick mark. Each tick mark to its right indicates a retraction of 0·10 of initial length. Dashed sections are below Instron sensitivity, but all reach zero stress at their known respective SC ratios. Species: 1, *A. diadematus*; 2, *A. marmoreus*; 3, *N. hentzii*; 4, *N. hentzii* (3 and 4 from the same spider); 5, *E. fuliginea*; 6, *A. aurantia*; 7, *E. ravilla*; 8, *E. ravilla* (7 and 8 from the same spider); 9, *A. argentata*; 10, *A. aurantia*; 11, *A. aurantia*; 12, *N. clavipes*; 13, *N. clavipes*; 14, *N. cruentata*.

Table 1, as are also the ratios of areas for those samples which supplied both curves. Moduli are measures of resistance to axial extension or expressions of axial stiffness, and, as such, are equal to the slopes of the tangents taken at any points on the curve. These moduli at initial lengths are given in Table 1, column 10.

Force-elongation of samples dried after SC

The force-elongation behaviour of MaAS that has been SC and then dried has been shown (idealized) in Fig. 1. Detailed examination of this subject is outside of the scope of this paper. However, it is pertinent to mention that the 'plateau of drawing', which takes place with little or no increase in force (stress) or related modulus, is always present. Also, this drawing is always completed before the samples arrive at their initial lengths, at which time the stress levels are two to three times those of the plateaux, with dynamic moduli increasing. As with the wet elongations, wide variability is found from sample to sample.

Dimensional recovery from small extensions

Little information is available on the viscoelastic performance of MaAS under conditions in which this material is used in the normal behavioural pattern of orb-web-building spiders. Denny (1976, Fig. 3) has pointed out that frame silk in webs made by *Nuctenea sclopetaria* (= *Araneus sericatus*) is in a condition of
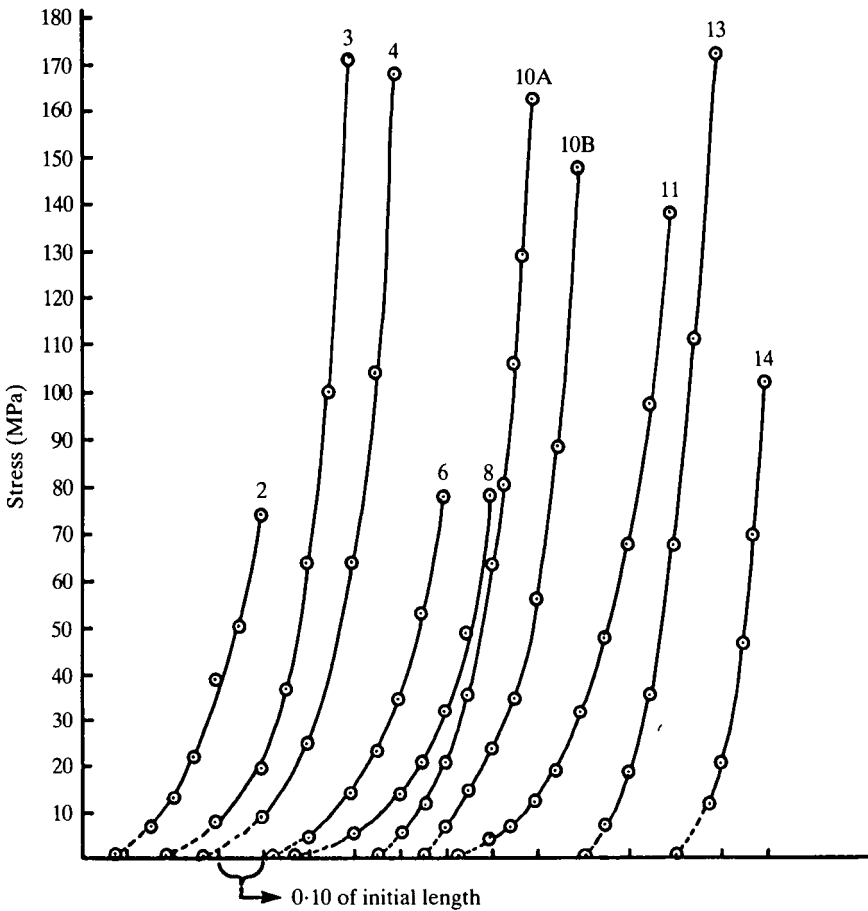
Fig. 4. Wet elongation from SC *versus* stress. Each curve ends at the initial length of the sample above a tick mark. Each tick mark to its left indicates an elongation equal to 0·10 of its initial length, starting from SC and finishing at initial length. Same samples and species identification as used in Fig. 3. 10A and 10B are adjacent samples.

extension of the order of 1 %. In the same paper he also reported upon the cyclical recovery of such silks from extensions of 10 % and greater. The former extension is below the 'yield' section of MaAS, and therefore in the essentially elastic 'Hookean' portion of the force-elongation curve. Extensions of 10 % or more are well above it, as may be seen in his paper.

Samples from a dragline made by an *Araneus diadematus*, subjected to a force equal to the spider's weight, elongated 1·8 % (2·2 s), gave a stress of 190 MPa. Similarly, one from a *Nuctenea cornuta* elongated 2·4 % (2·9 s), resulting in a stress of 220 MPa. In both cases the elongation curves were in the 'Hookean' sections, and upon immediate reversals of the crosshead these curves were retraced, as seen in curves 1Ad and 1Nc of Fig. 5. When these same strain levels were maintained for 1 min before release, the samples returned to their initial lengths as rapidly as

Table 1. *Stress (MPa), energy (arbitrary units) and moduli (GPa) of SC and wet re-extension of MaAS to the initial samples lengths*

1 No.	2 Species	3 SC ratio	4 Stress (MPa) at initial length Before SC	5 After SC	6 Ratio 5/4	7 Energy During SC	8 From SC	9 Ratio 8/7	10 Modulus (GPa)
1	A. diad.	0·64	32·5	—	—	1·08	—	—	—
2	A. mar.	0·57	24·5	74·0	3·02	1·04	2·55	2·45	—
3	B. hent.	0·58	30·4	170·3	5·60	1·28	4·99	3·90	2·16
4	N. hent.	0·57	20·4	168·7	8·27	0·66	5·24	8·0	1·27
5	E. ful.	0·64	18·	—	—	0·74	—	—	—
6	E. ful.	0·62	22·3	77·6	3·48	0·62	2·73	4·4	0·54
7	E. rav.	0·60	15·5	—	—	0·64	—	—	—
8	E. rav.	0·57	21·8	78·0	3·58	0·85	2·53	2·98	0·62
9	A. arg.	0·56	31·	—	—	0·84	—	—	—
10A	A. aur.	0·65	36·0	162·0	4·50	0·92	4·80	5·20	1·36
10B	A. aur.	0·65	—	147·0	—	—	4·49	—	1·42
11	A. aur.	0·54	44·5	137·7	3·09	1·17	5·52	4·72	0·97
12	N. clav.	0·67	31·	—	—	0·62	—	—	—
13	N. clav.	0·71	32·0	172·1	5·38	0·47	4·86	10·0	1·29
14	N. cru.	0·86	23·7	101·0	4·26	0·17	1·78	10·0	1·85
	All data		N=14	N=10		N=14	N=10		
	Mean		27·4	128·8		0·79	3·95		
	CV (%)		28·8	32·4		37·4	35·1		
	*		N=9	N=9	N=9	N=9	N=9	N=9	
	Mean		28·4	126·8	4·58	0·80	3·89	5·74	
	CV (%)		28·3	34·5	36·5	44·3	37·5	50·2	
	†		N=13	N=9		N=13	N=9		
	Mean		27·7	131·9		0·84	4·19		
	CV (%)		29·4	32·6		29·2	29·2		

*Samples having data in each of columns 4 to 9.
†Sample n.14 omitted.
CV, coefficient of variation.

the crosshead moved. But the closed hysteresis loop, seen in curve 2Ad, demonstrates that observable viscoelastic action takes place even in this short time. When the strain level was held for 5 min before being removed, zero tension was reached before the sample returned to its initial length, producing the open loop of curve 3Ad. When held in the Instron clamps, separated by a distance equal to the initial length of the sample, the sample was slack and bowed. It became straight in about 3 min, illustrating that elastic recovery was complete, but time delayed.

When elongation was increased to reach a tension equal to 1·5 times the spider's weight, the inflection section at the end of the Hookean section of the curve was just being exceeded at 2·7 % elongation, stress 330 MPa. The recovery curves were similar to curves 2Ad and 3Ad of Fig. 5, but the time factor was more apparent. In another experiment on a dragline sample from *N. cornuta*, the time to reach a force equal to the spider's weight was increased to 35 s, under which condition the 'Hookean' section developed curvature. When allowed to retract to zero tension, the sample was 2·0 % longer than initially and measurable stress developed within 1 min, as seen in curve 4Nc of Fig. 5. At a tension equal to twice
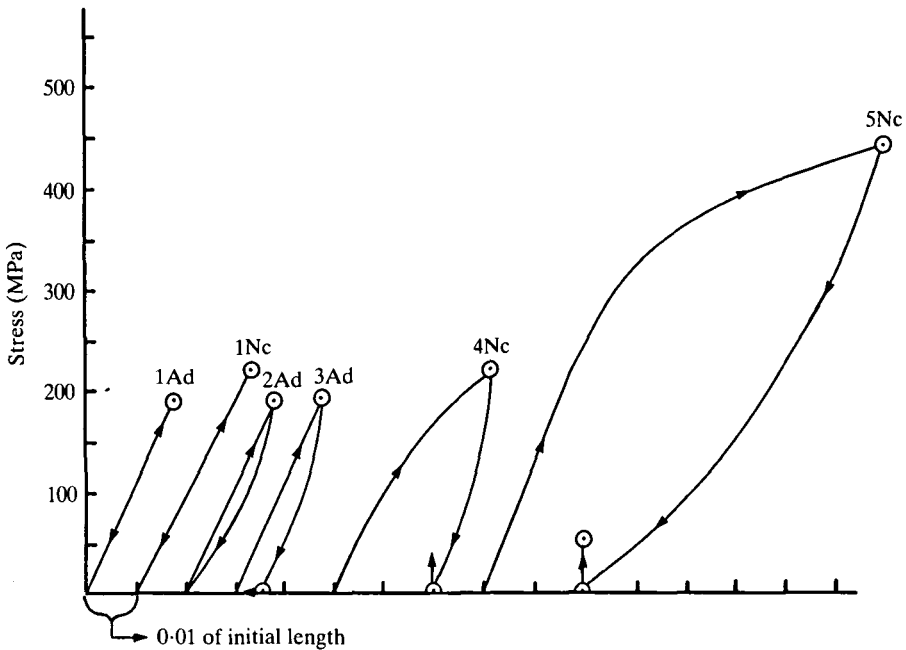
Fig. 5. Elongation and recovery from stresses related to those producible by the weights of the spiders, as functions of time. Each tick mark denotes 0·01 (1 %) elongation and retraction, based upon initial lengths of samples. Ad, *Araneus diadematus*; Nc, *Nuctenea cornuta*.

the spider's weight, the stress being 440 GPa, the yield section of the force-elongation curve had been passed, with the elongation reaching 8 %. Upon allowing contraction until the tension reached zero, the sample was 2·0 % longer than it was initially. When kept at this length, the stress increased to 50 MPa in 5 min. The internal retractive forces which produced this stress are the same as would have brought the sample back to its initial length, had this been allowed. Curve 5Nc of Fig. 5 shows this behaviour.

Stress relaxation

Based upon the known behaviour of viscoelastic fibres it would be expected that when MaAS are placed in strained states, the developed stresses would relax as logarithmic functions of time. Preliminary experiments showed this to be essentially the case, although small inflections might or might not occur after short time periods. Once past these, the regression curves related retained stress linearly to log time for periods up to a week. On this basis, experiments could be limited to periods of several thousands of seconds and thereby secure data from which satisfactory regression calculations could be made. The derived regression curves follow the simple expression:

$$\text{Stress (retained) (MPa)} = -\text{Slope (MPa)} \times \log \text{time (s)} + K,$$

where K equals the stress (MPa) at 1 s (log = 0), the hypothetical intersection.

Table 2 (samples wet) and Table 3 (samples dry) contain the data on the slopes (column 6) and constants (column 7), as well as other pertinent information. Regression curves illustrating some of these sets of data from Table 2 are seen in Figs 6 and 7, and from Table 3 in Figs 8 to 10. Statistical analyses were made, but references D-4, 5, 23, 27, 28, 38 and 39 (Table 3) were excluded for reasons that will be discussed later. The normalized stress retention ratios (column 8) allow comparisons to be made between data sets. Using Student's t-test, the following results were secured.

(1) Table 2, wet, before inflection ($N = 12$) showed a highly significant difference ($t = 5.09$, $P < 0.01$) from that after inflection ($N = 11$).

(2) Table 3, dry, before inflection ($N = 11$) showed a highly significant difference ($t = 3.66$, $P < 0.01$) from that after inflection ($N = 11$).

(3) Table 2, wet, before inflection ($N = 12$) was not significantly different ($t = 0.46$) from Table 3, dry, before inflection ($N = 11$).

(4) Table 2, wet, after inflection ($N = 12$) was not significantly different ($t = 0.03$) from Table 3, dry, after inflection ($N = 11$).

(5) Table 2, wet, no inflection ($N = 9$) was not significantly different ($t = 0.83$) from that before inflection ($N = 12$).

(6) Table 3, dry, no inflection ($N = 2$) could not be compared to that before inflection ($N = 11$) due to insufficient data for 'no inflection'.

Statistical analysis of the correlation coefficients: (column 9) gave the following results.

(1) Table 2, wet ($N = 22$), mean value = -0.9934, CV = 0.869 %.

(2) Table 3, dry ($N = 33$), mean value = -0.9906, CV = 1.641 %.

These mean values and CVs indicate a consistently good fit of regression curves to the data.

(3) Table 2, wet ($N = 22$) was not different from Table 3, dry ($N = 33$).

The data collected on stress developed during elastic memory experiments were examined in order to determine whether the stress-time relation could be represented by any simple equation. It was found that at the beginning of each experiment the stress was a direct, linear function of time, within the experimental limits already described. After about 200–500 s, the rate of stress development was found to be measurably decreasing and continued to decrease, even after tending to level off in the region of 2000–3000 s. This behaviour leads to the conclusion that the apparent linearity at the start may be an artifact due to the inability of securing adequately precise absolute measurements of tension. No satisfactory linearity could be provided to the regression curves by the application of logarithmic conversions of stresses or times, or both, for the stress-time relationships or sections of them. There is no reason, from a theoretical standpoint, why any such simple relationships should exist, and therefore it would be a mere mathematical exercise to develop polynomial equations to fit the data. Accordingly, the results are expressed as seen in Fig. 11.

Table 2. *Stress relaxation of MaAS, wet elongated from SC*

1	2	3	4	5	6	7	8	9	10	11
			Basis of							
Reference	No.	Species	stress	Time lapse	Slope	K	Ratio	CC	Moduli	SC ratio
W-1	1	*A. aur.*	SC–0·80	3–500	−1·5	19	0·919	−0·974	0·2	0·66
W-2	2A	*A. aur.*	SC–1·00	1–4096	−5·6	53	0·893	−0·998	0·5	0·60
W-3	1	*A. aur.*	SC–0·90	3–9200	−6·8	64	0·894	−0·996	0·6	0·66
W-4	3	*E. ful.*	SC–1·00	1–4096	−6·8	73	0·907	−0·994	0·5	0·71
W-5	4A	*N. hent.*	SC–0·95	1–64	−12·8	116	0·884	−0·997	0·8	0·51
W-6	4A	*N. hent.*	SC–0·95	128–6100	−7·5	104	0·928	−0·987	0·8	0·51
W-7	1	*A. aur.*	SC–1·03	3–80	−21·7	160	0·864	−0·996	1·3	0·66
W-8	1	*A. aur.*	SC–1·03	182–5640	−11·0	138	0·921	−0·997	1·3	0·66
W-9	2A	*A. aur.*	SC–0·90	1–2048	−1·5	20	0·925	−0·965	0·2	0·60
W-10	5A	*N. cru.*	SC–0·95	3–2280	−3·7	33	0·888	−0·993	1·0	0·86
W-11	3	*E. ful.*	SC–1·05	1–64	−13·9	140	0·900	−0·999	0·4	0·51
W-12	3	*E. ful.*	SC–1·05	128–7150	−10·0	133	0·926	−0·998	0·4	0·51
W-13	6A	*E. rav.*	SC–1·00	1–5500	−7·2	76	0·905	−0·995	0·4	0·51
W-14	5A	*N. cru.*	SC–1·00	3–2160	−9·1	99	0·908	−0·997	2·8	0·86
W-15	7	*N. clav.*	SC–1·00	1–64	−18·4	152	0·879	−0·994	1·3	0·70
W-16	7	*N. clav.*	SC–1·00	128–2096	−10·4	136	0·924	−0·971	1·3	0·70
W-17	2B	*A. aur.*	SC–1·00	1–64	−17·9	187	0·905	−0·999	1·0	0·60
W-18	2B	*A. aur.*	SC–1·00	128–4096	−8·2	168	0·951	−0·980	1·0	0·60
W-19	4A	*N. hent.*	SC–1·02	1–76 000	−15·2	202	0·925	−0·999	2·2	0·51
W-20	1	*A. aur.*	SC–1·05	3–80	−22·2	228	0·894	−0·998	1·7	0·66
W-21	1	*A. aur.*	SC–1·05	177–9500	−13·4	210	0·936	−0·998	1·7	0·66
W-22	5A	*N. cru.*	SC–1·09	3–60	−21·8	276	0·921	−0·998	4·4	0·86
W-23	5A	*N. cru.*	SC–1·09	122–3600	−15·4	267	0·942	−0·993	4·4	0·86
W-24	4A	*N. hent.*	SC–1·07	1–64	−26·1	273	0·905	−0·998	1·3	0·51
W-25	4A	*N. hent.*	SC–1·07	128–5000	−22·8	271	0·916	−0·955	1·3	0·51
W-26	2B	*A. aur.*	SC–1·10	1–32	−21·5	280	0·923	−0·998	3·4	0·60
W-27	2B	*A. aur.*	SC–1·10	64–8190	−15·6	272	0·943	−0·998	3·4	0·60
W-28	1	*A. aur.*	SC–1·10	3–80	−22·7	316	0·928	−0·998	2·0	0·66
W-29	1	*A. aur.*	SC–1·10	66–64 500	−15·5	303	0·949	−0·997	2·0	0·66
W-30	7	*N. clav.*	SC–1·10	1–32	−42·6	357	0·881	−0·999	2·1	0·70
W-31	7	*N. clav.*	SC–1·10	64–1024	−19·7	320	0·939	−0·995	2·1	0·70
W-32	5A	*N. cru.*	SC–1·15	3–123	−34·6	437	0·921	−0·998	5·8	0·86
W-33	5A	*N. cru.*	SC–1·15	243–1263	−20·6	408	0·949	−0·996	5·8	0·86
W-34	5A	*N. cru.*	SC–1·15	3240–10320	−30·5	440	0·931	−0·991	5·8	0·86

Column 1 gives a reference number for association of each data line with the text and curve in either Figs 6 or 7 (wet) or Figs 8–10 (dry).

Column 2 numbers the primary samples used. Where a single number is associated with more than one reference number in Table 2, as for example sample no. 1, this indicates that the sample was allowed to SC after a stress relaxation experiment, and re-used for the next higher level of extension. Where a letter is added to a number, i.e. samples 2A and 2B, of Table 2, and samples 2C, 2D, and 2E of Table 3, these identify adjacent initial samples taken from the same primary sample.

Column 3 identifies the species (abbreviated) of spiders that provided the samples. *A. aur.* = *Argiope aurantia*, *E. ful.* = *Eriophora fuliginea*, *N. hent.* = *Neoscona hentzii*, *N. cru.* = *Nephilengys cruentata*, *E. rav.* = *Eriophora ravilla*, *N. cla.* = *Nephila clavipes*, *N. corn.* = *Nuctenea cornuta*, *N. scl.* = *Nuctenea sclopetaria*.

Column 4 lists the basis of extension; examples, SC-0·80 means that the sample was elongated from supercontraction to 0·80 of its initial length; in Table 3, 1·00–1·01 indicates that the sample was elongated from its initial length to 1·01 thereof.

Column 5, time lapse, supplies information on the time periods (seconds) used in calculating linear stress-log time curves or sections of curves. Those for which the first section starts at 3 s or at 1 s were obtained by means of an older or a newer Instron, respectively.

Columns 6 and 7 provide slopes and constants for the calculated regression curves.

Column 8 gives constants which are the ratios of the retained stresses at the end of each decade of time, relative to the retained stresses at the start of the decades, calculated from the regression curves. For example, the datum 0·919, the first item in Table 2, column 8, shows that when the stress at 3 s is normalized to unity, the stress at 30 s is equal to 0·919 thereof. These ratios allow slopes of curves to be normalized for statistical analyses.

Column 9 supplies correlation coefficients (CC) for the relation between raw data used to calculate the regression curves and the linear curve thus obtained.

Column 10 gives the moduli of the Instron force-elongation curve at the point of maximum elongation, from which stress relaxation starts.

Column 11 supplies the SC ratio of the sample, i.e. the ratio of SC length to the initial length.

Table 3. *Stress relaxation of MaAS, dry elongated from SC*

1	2	3	4	5	6	7	8	9	10	11
Reference	No.	Species	Basis of stress	Time lapse	Slope	K	Ratio	CC	Moduli	SC ratio
D-1	5B	*N. cru.*	1·00–1·01	3–7600	−5·6	67	0·916	−0·909	7·9	0·86
D-2	2C	*A. aur.*	1·00–1·03	1–64	−16·2	110	0·852	−0·996	6·4	0·62
D-3	2C	*A. aur.*	1·00–1·03	128–2048	−13·1	104	0·875	−0·997	6·4	0·62
D-4	6B	*E. rav.*	1·00–1·02	1–8	−10·0	139	0·928	−0·995	1·3	0·51
D-5	6B	*E. rav.*	1·00–1·02	$16–8 \times 10^3$	−21·6	149	0·855	−0·996	1·3	0·51
D-6	6C	*E. rav.*	1·00–1·10	1–64	−17·9	145	0·876	−0·987	1·5	0·51
D-7	6C	*E. rav.*	1·00–1·10	$128–5 \times 10^3$	−7·8	126	0·938	−0·990	1·5	0·51
D-8	8A	*N. clav.*	1·00–1·02	1–64	−29·8	229	0·870	−0·999	2·6	0·58
D-9	8A	*N. clav.*	1·00–1·02	128–4096	−19·7	208	0·905	−0·987	2·6	0·58
D-10	5C	*N. cru.*	1·00–1·02	3–57	−12·0	102	0·883	−0·988	8·7	0·86
D-11	5C	*N. cru.*	1·00–1·02	117–4800	−4·7	89	0·947	−0·987	8·7	0·86
D-12	2D	*A. aur.*	1·00–1·15	1–32	−21·8	204	0·893	−0·997	1·7	0·62
D-13	2D	*A. aur.*	1·00–1·15	60–3800	−11·7	189	0·938	−0·995	1·7	0·62
D-14	9	*N. corn.*	1·00–1·20	1–64	−26·5	224	0·882	−0·999	2·6	0·52
D-15	9	*N. corn.*	1·00–1·20	128–7440	−11·7	200	0·941	−0·981	2·6	0·52
D-16	2E	*A. aur.*	1·00–1·20	1–32	−14·5	198	0·927	−0·996	0·9	0·62
D-17	2E	*A. aur.*	1·00–1·20	$64–4 \times 10^3$	−7·6	186	0·959	−0·998	0·9	0·62
D-18	4B	*N. hent.*	1·00–1·02	1–6480	−8·5	196	0·956	−0·998	1·7	0·51
D-19	5D	*N. cru.*	1·00–1·07	3–40	−24·4	267	0·909	−0·991	9·6	0·86
D-20	5D	*N. cru.*	1·00–1·07	80–900	−13·5	249	0·946	−0·995	9·6	0·86
D-21	5E	*N. cru.*	1·00–1·15	3–48	−40·6	490	0·917	−0·998	6·5	0·86
D-22	5E	*N. cru.*	1·00–1·15	108–1490	−30·0	476	0·937	−0·999	6·5	0·86
D-23	4C	*N. hent.*	1·00–1·10	1–64	—	—	—	—	2·8	0·51
D-24	4C	*N. hent.*	1·00–1·10	128–7680	−20·4	500	0·959	−0·997	2·8	0·51
D-25	5F	*N. cru.*	1·00–1·17	3–24	−47·5	568	0·916	−0·999	2·8	0·86
D-26	5F	*N. cru.*	1·00–1·17	48–1610	−22·6	532	0·957	−0·995	2·8	0·86
D-27	5F	*N. cru.*	1·00–1·17	2270–8300	−40·9	566	0·929	−0·983	2·8	0·86
D-28	8B	*N. clav.*	1·00–1·10	1–64	—	—	—	—	4·2	0·58
D-29	8B	*N. clav.*	1·00–1·10	128–2200	−22·7	493	0·954	0·991	4·2	0·58
D-30	10	*N. cru.*	1·075–1·094*	3–300	−43·7	545	0·920	−0·996	17·2	0·82
D-31	10	*N. cru.*	1·094–1·113	3–120	−42·2	610	0·931	−0·999	21·0	0·82
D-32	10	*N. cru.*	1·094–1·113	300–6300	−33·6	586	0·943	−0·999	21·0	0·82
D-33	10	*N. cru.*	1·113–1·132	3–48	−23·6	705	0·967	−0·997	21·0	0·82
D-34	10	*N. cru.*	1·113–1·132	120–9900	−39·6	727	0·945	−0·992	21·0	0·82
D-35	10	*N. cru.*	1·132–1·151	3–24	—	—	—	—	14·5	0·82
D-36	10	*N. cru.*	1·132–1·151	$24–15 \times 10^4$	−55·4	863	0·879	−0·965	14·5	0·82
D-37	10	*N. cru.*	1·151–1·17	Erratic behaviour.						
D-38	10	*N. cru.*	1·17 – Failed upon increasing strain level.							
D-39	**	*N. scl.*	1·00–1·21	10–5000	−83·6	1167	0·928			

See notes on Table 2.

*This sample had undergone four prior steps of elongation, 1·000 to 1·02 to 1·04 to 1·06 to 1·075, during a total elapsed time of about 25×10^4 s.

**Denny (1976), taken from his Figs 4 and 5, being smoothed curves.

DISCUSSION

No adequate theory has been developed to describe, certainly not to explain, what happens at the molecular level when MaAS supercontract. Changes in X-ray diffraction patterns are discussed by Work & Morosoff (1982) and birefringence by Fornes *et al.* (1983). On the basis of reduced birefringence, denoting a correspondingly lesser orientation of segments of the polypeptide chain
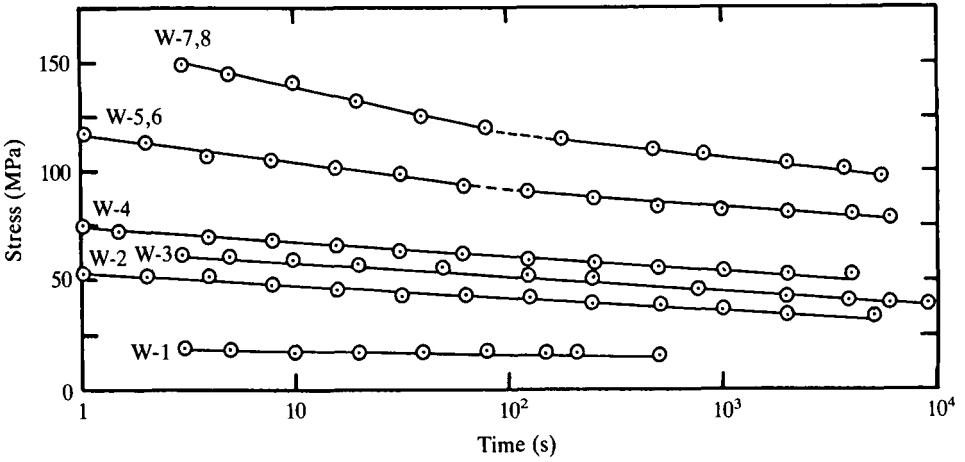
Fig. 6. Stress relaxation, see Table 2 and related text.
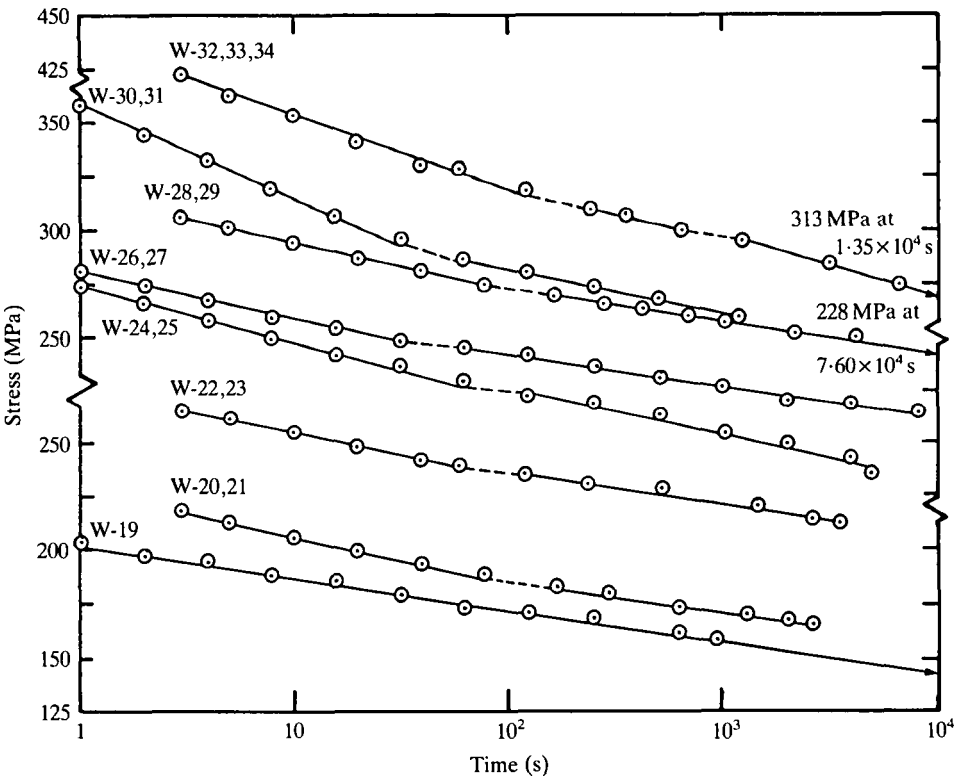

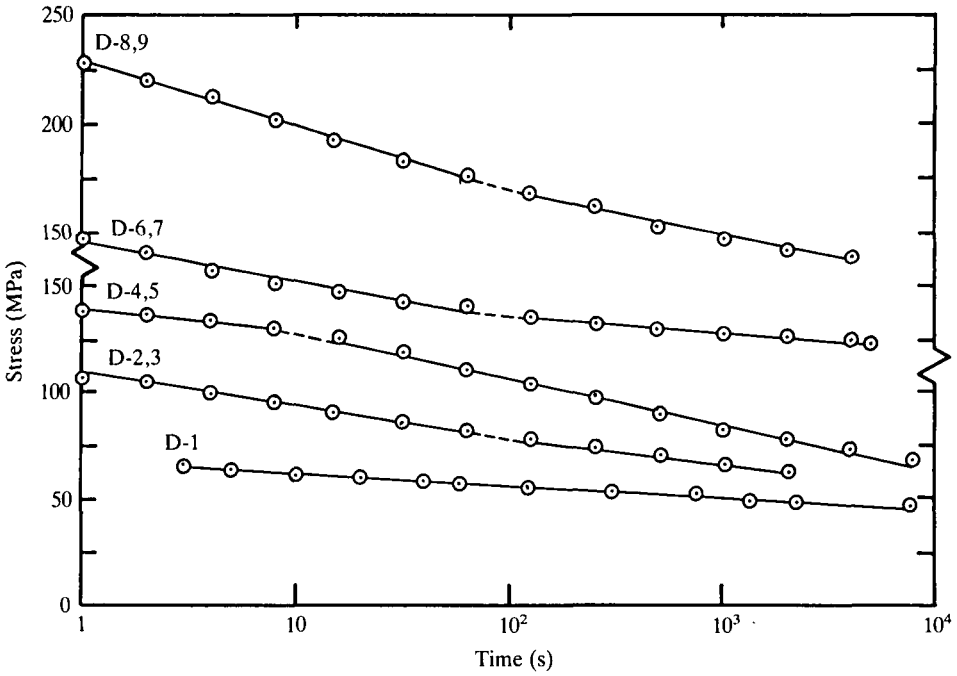Fig. 7. Stress relaxation, see Table 2 and related text.

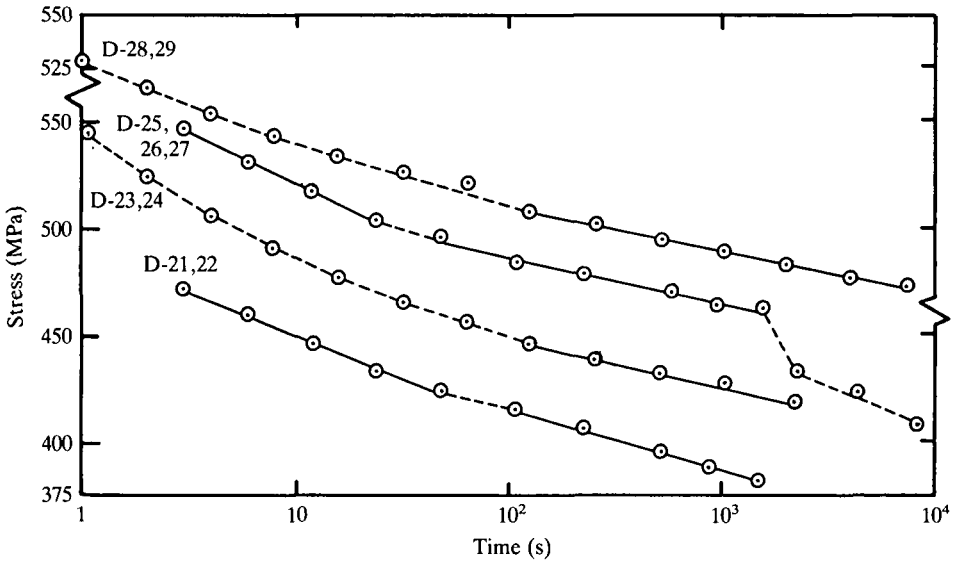Fig. 8. Stress relaxation, see Table 3 and related text.

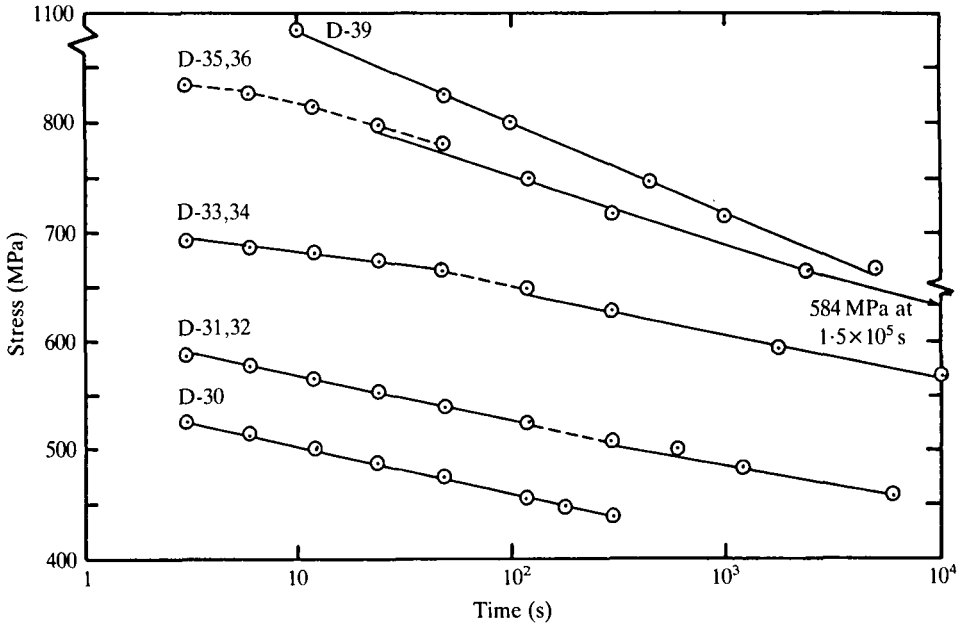Fig. 9. Stress relaxation, see Table 3 and related text.

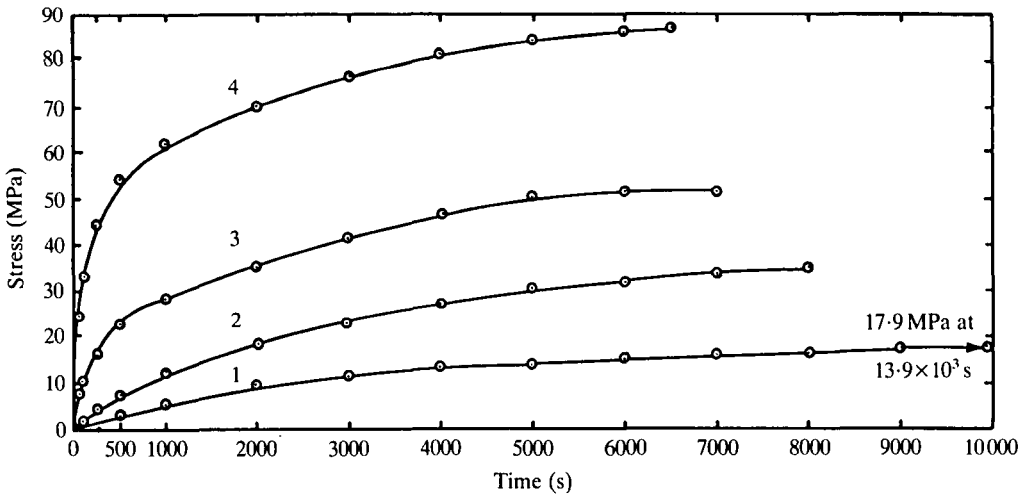Fig. 10. Stress relaxation, see Table 3 and related text.

Fig. 11. Elastic memory. 1 and 2, *Argiope aurantia*; 3, *Neoscona hentzii*; 4, *Nephila clavipes*.

molecules, the SC state can be said to be structurally ordered to a lesser degree than
prior to SC. But this does not connote an order-disorder transition during SC.
The combination of: (1) the observation that SC reaches a taxonomically related
SC ratio very rapidly and stops there (Work, 1981*b*), from where (2) the SC fibres
may be wet re-extended to initial lengths, and (3) conditions (1) and (2) may be
cycled repeatedly, suggests, in the author's opinion, that some manner of order
exists in the amorphous domains ('amorphous' is here used as meaning not

capable of giving an X-ray diffraction pattern) of the wet SC state. Beyond this, it is entirely conjectural as to whether the basis of SC may be either chain folding or the formation of helical conformations.

The development of potential energy when axially restrained MaAS are wetted, and subsequent SC if that restraint is removed, indicates that the normal dry MaAS is in a quasi-stable state. It is the wetted, SC state that is the only stable state from the standpoint of macromolecular chemistry. This refers, of course, to the entity known as major ampullate silk, and does not apply to the progenitive polypeptide, nor the transitory states (Work, 1977a) that are associated with its conversion to silk. It follows that after MaAS is produced, the wetted SC state is the zero energy state. Any sample secured by an experimenter is in a dynamic condition, wherein stress relaxation is occurring in a manner which has been quantified in this paper. But it is reasonable to depend upon the application of the Boltzmann Superposition Principle (1876), and accept that following some initial zero starting time, whatever strains that have been imposed, with consequent stress relaxations, do not change the fundamental nature of the response of MaAS to a strain imposed by an experimenter. This viewpoint has been adopted by the author, but it is also his opinion that some of the variability found among fibres from the same spider (Tables 2, 3; and Work, 1976, 1977b) may have resulted from their different histories.

Stress and energy in SC and re-extension

It has been seen in Table 1 that upon re-extension from SC to initial lengths, the mean stress was somewhat less than five times (with a large CV) of the stress developed in samples upon being wetted. The question arises as to whether this large difference in stress levels was caused by the stress relaxation that necessarily takes place between the time that the samples were produced by spiders and when they were subjected to measurements. In Table 2, the rates of change (slope) of stress retention are given for samples W-2 and W-4, these having been re-extended to initial lengths from SC. When it is calculated how long it would take for these stresses to drop to one-fifth of those which were present at 1 s, it is found that it would require 1·2 and 12·3 years, respectively. (At first glance this might be thought to be a great difference in time: it is only about one unit of log time.) Thus, although such extrapolations are far-fetched, they indicate that stress relaxation is not an adequate explanation for the wide differences found in stresses when MaAS are wetted at initial lengths, and those observed after SC and wet re-extension to initial lengths.

No conclusions of a taxonomic nature can be drawn from the data found in Table 1 and the curves illustrated in Figs 3 and 4, other than the obvious one that sample 14 from *Nephilengys cruentata*, with an SC of 0·86, differs from those with considerably lower SC ratios. Unfortunately, the trailing silk (presumably MaAS) from some uloborids, which also have SC ratios of about 0·84 (Work, 1981b), have diameters of less than 1·0 μm and were too small to be used in this study for comparison with MaAS from *N. cruentata*.

Dimensional recovery from small extensions

It was seen that samples of MaAS secured from draglines remained in the 'Hookean' sections of force-elongation curves, when these samples were subjected to forces equal to the weights of the donor spiders for time periods of short duration, such as might occur in dragline usage. Quantification of the viscoelastic 'creep' behaviour of MaAS under constant load, as these relate to spider weights, will depend upon the use of instruments which are operable at constant loads.

Stress relaxation

Based upon the statistical analyses of the data found in Tables 2 and 3, within the scope of the species included in this study, the stress relaxation behaviour of their MaAS is not related to taxonomy. In contrast, the amino acid and chemical compositions of MaAS are related to taxonomy (Fischer & Brander, 1960; Zemlin, 1968; R. W. Work, unpublished data). This implies that stress relaxation rates are uniform for chemically different polymers, a quite different situation from that which would be expected on the basis of the physico-chemical properties of man-made fibres. Among these materials, small differences in chemical composition usually produce wide differences in physical properties.

The relationships between stress retention and log time that do not exhibit inflections (Table 2, references W-1, 2, 3, 4, 9, 10, 11, 12, and Table 3, D-1 and D-18) were all based on relatively low absolute values of measured force. In contrast, two of those very high measured forces (Table 3, references D-23 and D-28) exhibited curvilinear behaviour before becoming linear at about 64 s. The others showed what appeared to be inflection sections in the time periods of about 60–100 s. It is reasonable to conclude that at the start of stress relaxation, the relationship between retained stress and log time may be slightly other than linear, but lack of precision in the measurement of small absolute forces may have prevented this property from being adequately defined.

It will be seen that the time-decade ratio for sample 6B (Table 3, reference D-4 and D-5, column 8) decreases after inflection, whereas with all other ratios, both dry and wet, with the exception of sample 10 (references D-30 to D-38 discussed below), this ratio increases. Examination of the original Instron curves for this sample and the one adjacent, 6C, showed that the former had not passed out of the 'Hookean' section. The latter did so, and then exhibited 'drawing', rather than the usual, immediate, increasing force. Thus, these samples had not been fully drawn by the spider in their production, a condition found in perhaps 3–4 % of primary samples secured during the several years of the broad study of MaAS.

Sample 10 was elongated, with subsequent stress relaxation, stepwise, to failure. At the strain level of 13·2 % (Table 3, references D-33 and D-34), the decade ratio (column 8) began to decrease and continued thereafter. Similarly, samples 5A (Table 2, references W-32, 33, 34) and 5F (Table 3, D-25, 26, 27) elongated to high levels of strain, showed a third section of stress relaxation

wherein the decade ratios declined. It is probable that these last two samples had entered a condition of incipient failure, similar to that found with sample 10.

In connection with all of the above described stress relaxation behaviour, it is appropriate to re-examine Denny's observations (1976), which are the basis of Table 3, reference 39. His smoothed curves (Figs 4, 5) do not exhibit inflections and the associated text mentions, '... at t 5000 s a plateau is reached' for Young's modulus, i.e. the slope of the stress relaxation curve. Both of these differ from the findings recorded in this paper, for which the following possible explanations are suggested.

(1) His early model Instron was calibrated at 4 g full scale and the fibres he used had cross sectional areas of an order of magnitude smaller than many of those available to the present study. It follows that the absolute magnitudes of tensions recorded on his Instron charts were very much smaller than those of the present study and therefore subject to conversion to correspondingly less precise final data.

(2) His curves are smoothed, with the raw data points not being indicated, and are plotted as log stress *vs* linear time, to give non-linear curves. Thus, the ease of noting small changes in slope of essentially linear curves was lost.

(3) His conclusion that the curve of his Fig. 4 reached a plateau in the time period 5000–10 000 s may possibly have been derived from the concept that this range, based on the use of linear time, was a very long one. It was, of course, equal to the entire preceding time period; but based upon log time it is only the range between 3·7 and 4·0 decades.

Elastic memory

It has already been noted that the Instron is not designed to provide the type of measurements that are involved in studies of elastic memory on MaAS. The data secured, however, confirm that MaAS behave as would be expected of viscoelastic fibres. The experiments may also provide some preliminary time-stress data, as the foundation for more extensive future studies.

Viscoelasticity, SC and the orb web

As a foundation for this discussion, it is appropriate to summarize the following background information.

(1) A major ampullate silk fibre evolves from a dynamic continuum of proto-polypeptide in the ampulla, through stages of water-reduction, development of birefringence, irreversible gellation, stretching (drawing), formation of crystalline domains (X-ray diffraction definition) and, after emergence from the major ampullate spigot, moisture equilibrium with the relative humidity of the ambient air (Work, 1977a). [See Iizuka (1966) for the corresponding formation of silk from *Bombyx mori*.]

(2) The final MaAS is labile to wetting by water, under which condition it swells radially and develops axially retractive tension (Work, 1977b).

(3) If axially unrestrained while wet, MaAS will SC to a level associable with taxonomy (Work, 1981*b*).

(4) In the SC condition, MaAS maintains a low level of optical birefringence (this being evidence of some retained molecular orientation, Work, 1977*b*), from which state it may be extended to its initial length and repeatedly cycled thereafter (this paper).

(5) If dried in the SC state and re-extended, MaAS undergoes a drawing stage, suggestive of the drawing of certain man-made fibres (Work, 1977*b*). This behaviour does not occur during wet stretching (this paper).

(6) Wet stretching to initial length from SC requires several times the amount of kinetic energy that is released as potential energy upon SC. This difference cannot be explained on the basis of stress relaxation (this paper).

(7) When extended in the wet condition from SC, or in the dry condition from initial length, the imposed strains produce stress levels from which relaxation takes place (this paper).

(8) Stress relaxation, both wet and dry, has been found to be quantifiable (as stress retention, equal to unity minus relaxation), essentially as linear functions of log time (this paper).

(9) At lower stresses (for example, those in the 'Hookean' region of dry extention), inflection may not occur at time periods in the region of 60–100 s, or the measured small levels of absolute tension may be inadequate to resolve inflections, if such exist (this paper).

(10) When tension levels are higher than those of item (9), and are measurable with increased certainty, inflections are found to occur in the region of 60–100 s, for both wet and dry conditions (this paper).

(11) Normalized rates of stress retention are not differentiable statistically, wet *vs* dry before inflection, or wet *vs* dry after inflection, but are differentiable before inflection *vs* after inflection in both conditions (this paper).

(12) Limited evidence indicates that the weights of spiders on their draglines produce stresses within the 'Hookean' sections of the dry force-elongation responses (this paper).

(13) After MaAS have been strained for long periods (hours to days) rapid reduction of strain sufficient to produce zero stress is reached at sample lengths greater than initial lengths (Benton, 1907), following which there is a continuing development of stress due to elastic memory (this paper).

(14) To the above items, based upon this and prior publications, the following need to be added. (a) When MaAS is forcibly taken (Work & Emerson, 1982), it very often rubs across a hair on one of the anterior spinnerets. When this happens, a droplet of liquid will be seen to accumulate at the point of contact. When this droplet is touched with a tiny tab of lens paper, rapid transfer occurs, in a manner typical of a liquid of low viscosity, such as water (unpublished observation). (b) It is estimated (Professor Ralph McGregor, personal communication) that for water-saturated MaAS of 2·5 μm diameter, an 80 % reduction in moisture will be reached in about 0·14 s, in 'an efficiently circulated air-stream'.

Turning now to the phenomenon of SC and the effects of viscoelasticity as these apply to MaAS in the orb web, let us start with an immobile spider, the condition in which it spends most of its time. The MaAS outside its body will be in equilibrium with the relative humidity of the ambient air; inside its body the continuum is liquid engulfed, with the entire glandular system at some minimum level of potential energy. If it is assumed that at some locus in the continuum there is a state analogous to the SC state, an attempt must be made to resolve the dilemma posed in item (6) above. Accordingly, it is possible to conjecture that a natural process will seek and become operated at the lowest possible level of energy usage. It is suggested that the body fluid (of unknown pH, inorganic ion and other chemical content) facilitates the final step in the α–β conversion in a manner not achievable with distilled water, as used in the experiments.

A dynamic sequence of events occurs when the newly generated MaAS emerges from the spigot into the air. Factors affecting its drying will include fibre radii, time of exposure to air, relative humidity and air velocity at the fibre surfaces, to mention only four obvious ones. Additionally, this transition from moisture saturation to dryness is carried out under the tension necessary to complete the α–β conversion and stretch the resulting MaAS to its final physical form. Perhaps the only definitive thing that can be said of the magnitude of this tension is that the weight of the spider is adequate to achieve this end. Wilson (1962, Table 3) forcibly silked 'lightly etherized adult female *Araneus*' (*diadematus*) spiders at forces ranging from 4 to 65 mg (mean = 31 mg, CV = 64 %, N = 14 measurements, author). Although the weights of the spiders were not stated, even the maximum tension is far smaller than the usual weights of these spiders.

Eberhard (1981, Fig. 2 and related text) has reported that the tension decreases during the formation of radii of orb webs. (Although the caption to the figure states that '... spiders usually reduce tensions on new radii ...', the related text clearly indicates that it is the viscoelastic property of the material, not the physical control provided by the spider, that brings about the decrease in tension.) The magnitude of this decrease may be considered in the light of the rates of stress relaxation seen in Tables 2 and 3. Although these apply to static systems, rather than to the dynamic conditions present during MaAS formation, the present study is in complete agreement with his observations.

The same author (Eberhard, 1981, Fig. 3) showed that a spider may move on two sides of a triangle to place a radius that becomes its third side, which must be shorter than the distance it has travelled; i.e. potential slackness must exist in its production. At any time when any part of it is still wet and is allowed to become slack, SC will bring about axial shrinkage. That this type of SC shrinkage does occur, indeed may be less than rare, is supported by other evidence, one example of which has already been mentioned in this paper, in which it was pointed out that the force-elongation curve of sample 6C had displayed a short drawing plateau. This indicated that either it had never been completely drawn or had been allowed to SC to a limited degree after being drawn.

A second clue is found in the association of MaAS with minor ampullate silk

fibres (MiAS). Although the function of the latter silk in the orb web has not been defined, it is almost invariably found with the former silk. The MiAS possesses viscoelastic properties similar to those of MaAS, but it does not SC when wetted (Work, 1978b, Table 1, Fig. 2, and associated text). When the two are found in samples, they are more often than not in line contact for their entire lengths. But a considerable number of MiAS pairs are found to loop slightly away from the MaAS pair (see Jackson, 1971, Fig. 2C; Kavanagh & Tillinghast, 1979, Fig. 6; Work, 1981a, Fig. 17B). Careful separation of the two pairs shows that the MiAS may be as much as 5 % longer than the MaAS. It is a reasonable conclusion that the two pairs were originally of the same length, i.e. the distance travelled by the spider during their generation. But if the movements of the spider allowed any slack to occur while the two pairs were still wetted, the MaAS pair would instantly SC until it became taut, buckling the smaller MiAS in so doing. It is possible that this same behaviour, not confirmable when the MaAS are not found associated with MiAS, may be quite common and account for some of the variability reported for SC ratios, for example, the CV of 13·6 % (Work, 1981b, Table 1) for 41 samples from 18 *Araneus diadematus* spiders. Indeed, the amount of stretching from some hypothetical zero energy state, similar to the SC state reported in this paper, and the degree of axial retraction, if any, that takes place during web building, may be the basis of the wide variability found in the force-elongation properties (Work, 1976) of MaAS from orb webs. The presence of SC in MaAS, the lack of it in MiAS, and the viscoelastic behaviour of all structural elements of orb webs, warrant further study.

REFERENCES

ANDERSEN, S. O. (1970). Amino acid composition of spider silks. *Comp. Biochem. Physiol.* **35**, 705–711.

ASTBURY, W. T. & WOODS, H. J. (1933). X-ray studies of the structure of hair, wool and related fibres. II. The molecular structure and elastic properties of hair keratin. *Phil. Trans. R. Soc. Ser. A.* **232**, 333–394.

BENTON, J. R. (1907). The strength and elasticity of spider threads. *Am. J. Sci.* **24**, 75–78.

BOLTZMANN, L. (1876). Zur Theorie der Electrischen Nachwirkung. *Ann. Physik. Erg. Bd* **7**, 624–654.

BRAUNITZER, G. & WOLFF, D. (1955). Vergleichende Chemische Untersuchungen über die Fibroine von *Bombyx mori* und *Nephila madagascariensis. Z. Naturf.* **10**, 404–408.

CHABERT, B., NÉMOZ, G. & VALENTIN, N. (1979). Study of the contraction and crystallization phenomena during thermal treatments of preoriented polyester yarns. *Bull. Sci. Inst. Textile Fr.* **8**, 53–66.

DENNY, M. (1976). The physical properties of spider's silk and their role in the design of orb-webs. *J. exp. Biol.* **65**, 483–506.

DE WILDE, J. (1943). Some physical properties of the spinning threads of *Aranea diadema L. Archs. néerl. Physiol.* **27**, 117–132.

EBERHARD, W. G. (1981). Construction behaviour and the distributions of tensions in orb webs. *Bull. Br. Arachnol. Soc.* **5**, 189–204.

EBERT, G., EBERT, C. & WENDORFF, J. (1970). Fibrous keratins. 15. Chemical and physical investigations of fibrous keratins. Influence of internal and external parameters on the supercontraction. *Kolloid, Z. Z. Polym.* **237**, 229–251.

FERRY, J. D. (1969). Viscoelasticity. In *Encyclopedia of Polymer Science and Technology*, Vol. 14, (ed. N. M. Bikales), pp. 670–717. New York: Interscience Publishers.

FISCHER, E. (1907). Uber Spinnenseide. *Z. physiol. Chem.* **53**, 126–139.

FISCHER, F. G. & BRANDER, J. (1960). Eine Analyse der Gespinste der Kreuzspinne. *Hoppe-Seyler's Z. physiol. Chem.* **320**, 92–102.

FITZGERALD, T. D. & WILLER, D. E. (1983). Tent-building behaviour of the eastern tent caterpillar *Malacosoma americanum.* (Lepidoptera: Lasiocampidae). *J. Kans. ent. Soc.* **56**, 20–31.

FORNES, R. E., WORK, R. W. & MOROSOFF, N. (1983). Molecular orientation of spider silks in the natural and supercontracted states. *J. Polym. Sci., Polym. Phys. Ed.* **21**, 1163–1172.

HERZOG, A. (1915). Zur Kenntnis der Spinnenseide. *Kunststoffe* **5**, 25–27, 53–55.

IIZUKA, E. (1965). Degree of crystallinity and modulus relationships of silk thread from cocoons of *Bombyx mori L.* and other moths. *Biorheology* **3**, 1–8.

IIZUKA, E. (1966). Mechanism of fiber formation by the silkworm, *Bombyx mori L. Biorheology* **3**, 141–152.

JACKSON, R. R. (1971). Fine structure of the thread connections in the orb wèb of *Araneus diadematus. Psyche* **78**, 12–31.

KARGIN, V. A. & SLONIMSKY, G. L. (1968). Mechanical properties. In *Encyclopedia of Polymer Science and Technology*, Vol. 7, (ed. N. M. Bikales), pp. 445–516. New York: Interscience Publishers.

KAVANAGH, E. J. & TILLINGHAST, E. K. (1979). Fibrous and adhesive components of the orb web of *Araneus trifolium* and *Argiope trifasciata. J. Morph.* **160**, 17–32.

KO, F. F. (1976). Nonlinear viscoelasticity of polyamide fibers. Ph. D. dissertation, Georgia Institute of Technology, Atlanta, Georgia, U.S.A.

LEADERMAN, H. (1943). *Elastic and Creep Properties of Filamentous Materials and Other High Polymers.* Washington, D.C.: The Textile Foundation.

LUCAS, F. (Jan., 1964). Spiders and their silks. *Discovery*, 8 pp.

LUCAS, F., SHAW, J. T. B. & SMITH, S. G. (1955). V. The chemical constitution of some silk fibroins and its bearing on their physical properties. *J. Text. Inst.* **46**, T440–T452.

LUCAS, F., SHAW, J. T. B. & SMITH, S. G. (1958). The silk fibroins. In *Advances in Protein Chemistry*, Vol. 13, (ed. C. B. Anfinsen, JR.), pp. 107–242. New York, London: Academic Press.

LUCAS, F., SHAW, J. T. B. & SMITH, S. G. (1960a). Comparative studies of fibroins. I. The amino acid composition of various fibroins and its significance in relation to their crystal structure and taxonomy. *J. molec. Biol.* **2**, 339–349.

LUCAS, F., SHAW, J. T. B. & SMITH, S. G. (1960b). The composition of anthropod silk fibroins. XI Int. Kongr. f. Entom., Wien 1960. Verh. B III, 208–214. *Verlag. Inst. Ent. Univ.* Pavia.

MELINTE, S., LEANCA, M., MOISE, M. & MATEESCU, N. (1977). Interdependence between structure and thermal contraction of some poly(ethylene terephthalate) (PET) filaments. *Bul. Inst. Politeh. Iasi.* Sect. 1. 23, 105–109 (via *Chem. Abst.* 90–40052).

PAULING, L. & COREY, R. B. (1951). Configurations of polypeptide chains with favored orientations around single bonds: two new pleated sheets. *Proc. natn. Acad. Sci. U.S.A.* **37**, 729–740.

PAULING, L. & COREY, R. B. (1953). Two rippled sheet configurations of polypeptide chains, and a note about the pleated sheets. *Proc. natn. Acad. Sci. U.S.A.* **39**, 253–256.

PEAKALL, D. B. (1964). Composition, function and glandular origin of the silk fibroins of the spider *Araneus diadematus* Cl. *J. exp. Zool.* **156**, 345–352.

PEAKALL, D. B. (1968). Specificity of the web. In *A Spider's Web. Problems in Regulatory Biology*, (eds P. N. Witt, C. F. Reed & D. B. Peakall), pp. 5–16. New York: Springer-Verlag.

PREVORSEK, D. C., TIRPAK, G. A., HARSET, P. J. & REIMSCHSIESSEL, A. C. (1974). Effects of thermal contractions on structure and properties of PET [poly(ethylene terephthalate)] fibers. *J. Macromol. Sci., Phys.* **9**, 733–759.

REBENFELD, L. (1967). Fibers. In *Encyclopedia of Polymer Science and Technology*, Vol. 6, (ed. N. M. Bikales), pp. 505–573. New York: Interscience Publishers.

SPEAKMAN, J. B. (1931). The action of sodium sulphide on wool. *J. Soc. Chem. Ind.* **50**T, 1–7.

UCHIYAMA, S. & YAMAMOTO, T. (1972). Poly(ethylene terephthalate) fibers with high contractibility. Japanese Patent 72 14,055 (via *Chem. Abst.* 77–141401).

WAINWRIGHT, S. A. (1976). Principles of the strength of materials: phenomenological description. In

Mechanical Design in Organisms, (eds S. S. Wainwright, W. D. Biggs, J. B. Currey & J. M. Gosline), pp. 6–44, 353–354. New York: John Wiley & Sons.

WARWICKER, J. O. (1954). The crystal structure of silk fibroin. *Acta Crystallogr.* **7**, 565–573.

WARWICKER, J. O. (1955). The crystal structure of silk fibroins. *Faraday Soc. Trans.* **52**, 554–557.

WARWICKER, J. O. (1960). Comparative studies of fibroins. II. The crystal structures of various fibroins. *J. molec. Biol.* **2**, 350–362.

WEBER, W. (1835). Über die Elasticity der Seidefäden. *Ann. Phys.* **34**, 247–257.

WHEWELL, C. S. & WOODS, H. J. (1946). The supercontraction of animal fibres. *Soc. Dyers Colourists, Sym. on Fibrous Proteins*, 50–57.

WILSON, R. S. (1962). The control of dragline spinning in the garden spider. *Q. J. microsc. Sci.* **104**, 557–571.

WORK, R. W. (1976). The force-elongation behavior of web fibers and silks forcibly obtained from orb-web-spinning spiders. *Textile Res. J.* **46**, 485–492.

WORK, R. W. (1977a). Mechanisms of major ampullate silk fiber formation by orb-web-spinning spiders. *Trans. Am. microsc. Soc.* **96**, 170–189.

WORK, R. W. (1977b). Dimensions, birefringences, and force-elongation behavior of major and minor ampullate silk fibers from orb-web-spinning spiders. The effects of wetting on these properties. *Textile Res. J.* **47**, 650–662.

WORK, R. W. (1978). Mechanisms for the deceleration and support of spiders on draglines. *Trans. Am. microsc. Soc.* **97**, 180–191.

WORK, R. W. (1981a). Web components associated with the major ampullate silk fibers of orb-web-building spiders. *Trans. Am. microsc. Soc.* **100**, 1–20.

WORK, R. W. (1981b). A comparative study of the supercontraction of major ampullate silk fibers of orb-web-building spiders (Araneae). *J. Arachnol.* **9**, 299–308.

WORK, R. W. (1984). Duality in major ampullate silk and precursive materials from orb-web-building spiders (Araneae). *Trans. Am. microsc. Soc.* **103**, 113–121.

WORK, R. W. & EMERSON, P. D. (1982). An apparatus and technique for the forcible silking of spiders. *J. Arachnol.* **10**, 1–10.

WORK, R. W. & MOROSOFF, N. (1982). A physico-chemical study of the supercontraction of spider major ampullate silk fibers. *Textile Res. J.* **52**, 349–356.

ZEMLIN, J. C. (1968). A study of the mechanical behavior of spider silks. Technical Report 69-29-CM, AD 684333, U.S. Army Natick Laboratories, Natick, MA, U.S.A.